COBEM 99
XV Congresso Brasileiro de Engenharia Mecânica
15th Brazilian Congress of Mechanical Engineering
22 - 26 de Novembro de 1999 / November 22 - 26, 1999 Águas de Lindóia, São Paulo,

FAST HYDRAULIC AND MAGNETIC ACTUATORS FOR MECHANICAL ENGINEERING APPLICATIONS

Heinz Ulbrich
University of Essen, FB 12 - Institute of Mechanics
D - 45117 Essen, Germany
Phone: ++49/201/183-3283, Fax: ++49/201/183-2871
ulbrich@uni-essen.de

Abstract. *The realisation of actively controlled mechanical engineering systems requires suitable actuators. The paper deals with the design, modelling and practical realisation of two linear actuators - a hydraulic and an electromagnetic one – taking the required features above as a guideline. The hydraulic actuator on the one hand consists, essentially, of a lower and an upper body being elastically connected to each other by two annular membranes. These membranes form chambers in which an oil pressure can be controlled by a commercial servo valve. This avoids the typical disadvantages of ordinary hydraulic cylinders - which are leakage, body friction, a rather extended length and low stiffness - and leads to a new actuator type with a very compact design and good transfer characteristics. The magnetic actuator on the other hand consists of two pot-shaped magnets in which control coils are integrated. Here too, membranes are used for a frictionless linear guidance of the regulating motion. The suitable integration of high level permanent magnets - which provide the bias-flux - is shown to be crucial for the maximum realisable control force. Different design criteria are discussed. Theoretical and experimental results will be given for both actuator types. Their advantages and disadvantages as well as some future aspects will be discussed.*

Keywords: *actuators, electromagnetic, hydraulic, servo valve, membranes, permanent magnets, modelling, experiment.*

1. INTRODUCTION

The key to successful active control of the dynamics of mechanical engineering systems lies in the availability of suitable actuators. In mechanical engineering, most applications require minimum size actuators that generate forces in the kN-range with frequencies up to 500 Hz and displacements in the mm-range. Hence, especially electromagnetic, hydraulic and piezoelectric actuator systems are suitable. Apart from the wide spread use of magnetic bearings in rotor dynamics, linear motion piezoelectric actuators are commonly used in mechanical engineering. They lead to good results when only small regulating distances in the μm-

Note: Permission to publish this paper was given by the editor of [1].

range are demanded. However, if high forces (kN-range) and displacements in the mm-range are to be generated, actuators based upon magnetic or hydraulic principals tend to be superior to piezo actuators. The paper presents two actuators, a hydraulic and an electromagnetic actuator, whose performance data indicate their good feasibility for applications in mechanical engineering. Parts of the paper are already published in [1].

2. HYDRAULIC ACTUATOR

First, it is presented a hydraulic actuator that has a significantly better transfer characteristic than conventional actuators with piston-cylinder configurations. Due to its special design, the influence of friction is reduced and the stiffness increased. Some basic ideas towards the development of such an actuator have already been proposed in [2]. A sketch of the working principle and a prototype of the actuator under consideration are shown in Figure 1.

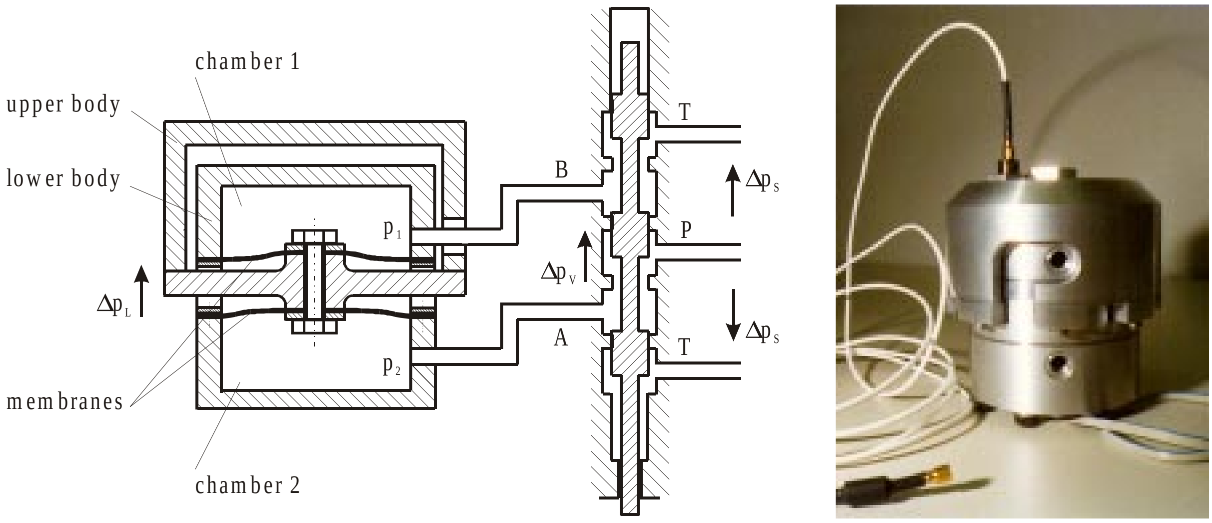

Figure 1- Sketch and prototype of the hydraulic actuator.

The main parts of the hydraulic actuator are two bodies connected by two annular membranes, that provide the necessary axial flexibility together with a high radial stiffness. By this design, two oil chambers are formed. The regulating forces arise from the oil pressure difference between the two chambers and can be controlled with a servo valve. Whereas, due to friction and a low stiffness, common hydraulic cylinders have certain drawbacks with respect to their dynamic behaviour, these disadvantages can be avoided by the chosen design that constitutes a compact actuator with good transfer characteristics.

The membranes are the key elements of the actuator system: Given the desired maximum control force for the whole operating range F_{max}, the maximum control distance x_{max}, the maximum oil pressure within the chambers $p_{k,max}$ and the outer diameter of the membranes d_A, the remaining design parameters are the inner diameter of the membranes d_I and the membrane thickness t. The result of a corresponding parameter variation is given in [3]. The actuator shown in Figure 1 has an outer diameter of the membranes of 100 mm and provides regulating forces up to 20 kN and displacements up to $\pm$ 0.5 mm. The input pressure at the servo valve was chosen to p_s = 170 bar, the maximum pressure within the oil chambers (output pressure of the servo valve) is limited to $p_{v,max}$ = 70 bar.

For monitoring and control purposes, various sensors can be integrated: A displacement sensor for monitoring the regulating motion, strain gages for controlling the stress in the membranes and pressure sensors for measuring the pressures in the oil chambers (and thus the control force). The controller is implemented on a DSP board which allows to compensate nonlinearities and to realise problem-oriented control concepts.

The dynamics of the hydraulic actuator can be represented by the differential equation

$$K^* \cdot \Delta\dot{p}_k + K_{pq} \cdot \Delta p_k + K_R \cdot c_t \cdot \dddot{x}_L + K_{pq} \cdot c_t \cdot \ddot{x}_L + A^* \cdot \dot{x}_L = \sqrt{\frac{\Delta p_s}{\Delta p_N}} \cdot Q(u(t)) \,. \tag{1}$$

Here, K* denotes the effective compressibility (regarding the oil compressibility as well as the elasticity of the oil pipes and the membranes at a fixed position), K_{pq} the leakage factor, A^* the characteristic membrane area, K_R accounts for the compressibility of the oil within the oil pipes, c_t accounts for the inertia of the oil and Δp_s and Δp_N denote pressure differences depending on the choice of the servo valve. The servo valve output Q[u(t)] is a function of the control voltage u(t) and the dynamical behaviour of the servo valve which, according to the manufacturer, can be described by a PT_2-characteristic [4]. The pressure difference between the chambers Δp_k and the regulating distance x_L are related to each other by the control force F^*:

$$F^*(t) = A^* \Delta p_K(t) - 2c_F x_L(t) \,, \tag{2}$$

where c_F is the effective membrane stiffness. For the moving masses in the experimental setup [3] the momentum principle yields

$$F^*(t) = m\,\ddot{x}_L(t) \,. \tag{3}$$

From equations (1)-(3) the transfer characteristic for the regulating distance $x_L = x_L(\Omega)$ can be calculated. Figure 2 shows in a Bode-plot for the regulating distance that theory and measurement are in good agreement up to 150 Hz. The increasing deviations beyond 150 Hz are due to the neglection of further dynamic effects.

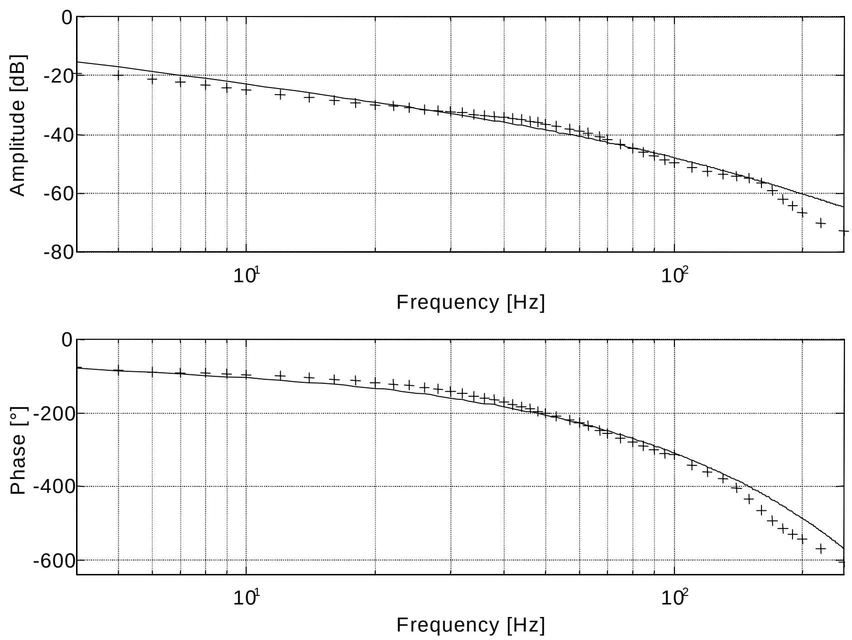

Figure 2- Transfer characteristics of the regulating distance:
simulation (——); measurement (+++).

The phase response at higher frequencies can be critical for certain practical applications. However, in the simulation of an active vibration isolation excellent results have been obtained for frequencies up to 50 Hz using a learning feed forward control [5]. In order to improve the actuator's phase response at higher frequencies, e.g. the length of the oil pipes could be reduced. Thus, a significant improvement of the phase response had been accomplished when the length was reduced from 2 m to 0.5 m (Figure 3); i.e. the best phase response will be obtained when the oil pipes are as short as possible. This suggests the integration of the servo valve into the actuator. Also, improvements are expected from the development of new high-response servo-valves.

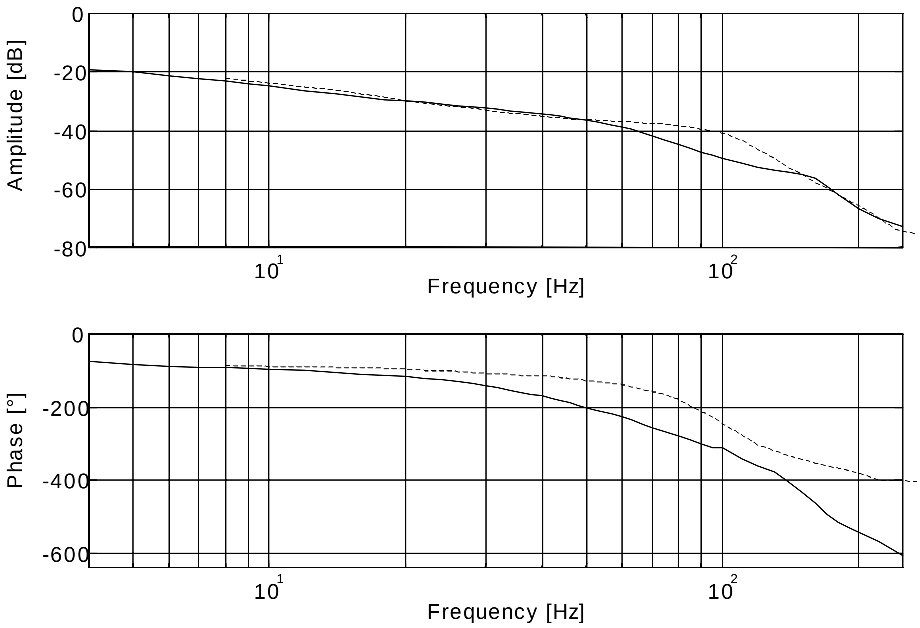

Figure 3- Measured transfer characteristic of the regulating distance for various length of the oil pipes: 2 m (——), 0.5 (---).

3. MAGNETIC ACTUATOR

Various magnetic actuator systems have been developed [6]. They differ mainly with respect to the pre-magnetisation (bias-flux) which can be realised either by coil systems or by permanent magnets which are integrated either in the core or in the pull disk of the actuator. Investigations showed that the pre-magnetisation method has a significant influence on the actuator's performance. One promising actuator concept will now be explained in more detail. A sketch of the working principle and a prototype are shown in Figure 4.

Between two magnetic heads, each with an integrated control coil, the axis with the pull disk is radially supported by two annular membranes. The current through the control coil generates magnetic flux and thus magnetic attractive forces acting on the pull disk. Additionally to this magnetic control field, a high energy pre-magnetisation circuit (bias-flux) is superimposed whose field is generated by permanent magnets that are integrated like a ring into the pull disk. The control coils are configured as to increase the magnetic field on one side (in axial direction) of the pull disk and decrease it on the opposite side (differential principle). Hence, a directional control force is generated along the amplified magnetic field. The positive correlation between the magnetic forces and the regulating distance (i.e. negative stiffness) is reduced by the spring characteristic of the membrane support along the moving axis; yet it might have to be further compensated by an internal feedback control. The membranes, moreover, provide at the same time a stiff radial support together with a friction-free motion in axial direction.

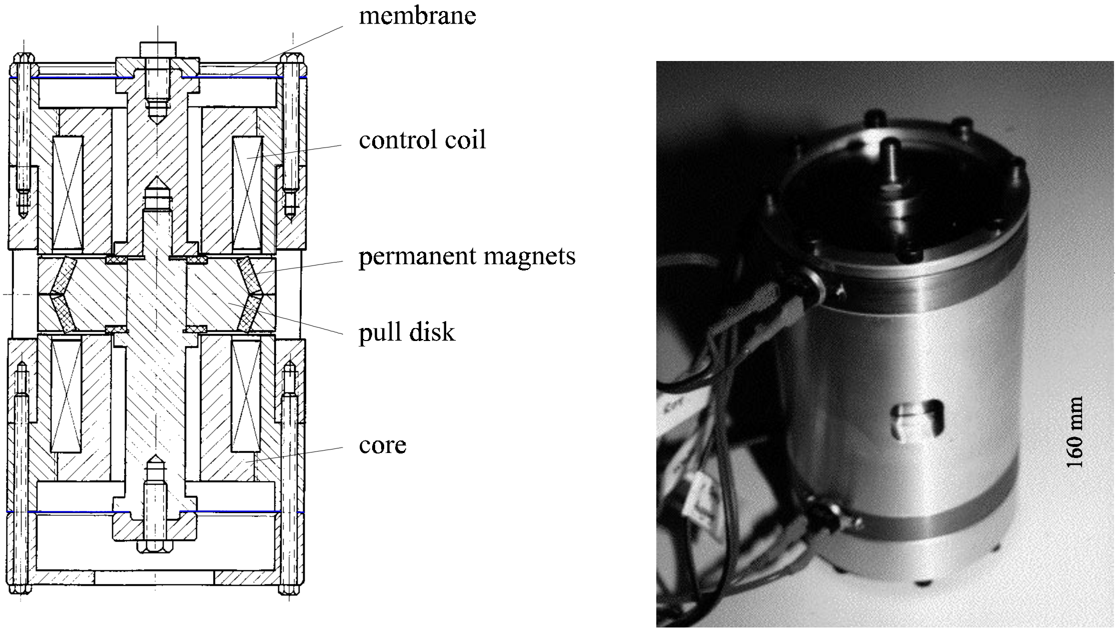

Figure 4- Sketch and prototype of the magnetic actuator.

During the design process, several parameters have to be determined such as the materials and dimensions of the coil windows, the core areas and the membranes. All of these parameters have to be carefully chosen with respect to the required performance data including the control distance, force and frequency as well as the actuator’s size. The attainable control distances and forces strongly depend on the membrane geometry, the characteristic properties of the membrane material (Young’s modulus, permissible stress) and the feasible magnetic fields (generated by permanent magnets and coil systems). The design and the calculation of the magnetic circuits is covered in [6] in great depth. The attainable control force F_m of the actuator is given in [6] for the quasi-static case as a function of the control distance x, the magnetic flux $\Theta_{St} = i\, w$ due to the control current (w: number of loops in the coil) and all of the geometric, electric and magnetic parameters:

$$F_m = \frac{1}{k_{mf}^2}\left\{\left[4k_f(1-\sigma)^2\left(\Theta_{pm}^2+\Theta_{St}^2\right)x_0 + \frac{8l_{pm}\Theta_{St}^2(1-\sigma)}{\mu_0\mu_{pm}A_{pm}}\right]x + \left[4k_f(1-\sigma)^2\left(x_0^2+x^2\right)\Theta_{pm} + \frac{8l_{pm}\Theta_{pm}x_0(1-\sigma)}{\mu_0\mu_{pm}A_{pm}}\right]\Theta_{St}\right\} \tag{4}$$

with

$$k_{mf} = \frac{2l_{pm}x_0}{\mu_0\mu_{pm}A_{pm}} + (1-\sigma)\left(x_0^2-x^2\right)k_f \quad , \quad k_f = \frac{1}{\mu}\left(\frac{1}{A_{ik}}+\frac{1}{A_{ak}}\right)$$

and the chosen denotations of the parameters and the numeric data is given in Table 1.

Table 1. Parameters and numerical data of the magnetic actuator

Dispersion coefficient	σ	$\approx$	0.5
Magnetic flux due to permanent magnets	Θ_{pm}	=	7640A
Magnetic flux due to control current	$\Theta_{St,max}$	=	1165A
Prescribed air gap between pull disk and core area	x_0	=	1mm
Thickness of the permanent magnets ring	l_{pm}	=	4.3mm
Cross section area of the permanent magnets ring	A_{pm}	=	4080mm^2
Relative permeability of steel	μ_{Fe}	=	1000
Magnetic field constant	μ_0	=	$4\,\pi\,10^{-7}\Omega s$
Cross section area of inner core	A_{ik}	=	1256mm^2
Cross section area of outer core	A_{ak}	=	1178mm^2

As can be seen from (4), the relationship between the control force F, the control current and the control distance x is nonlinear. If

$$\Theta_{St} << \Theta_{pm} \quad \text{and} \quad x << x_0 \ ,$$

(4) can be transformed to

$$F_m = k_x x + k_i i \quad , \tag{5}$$

where

$$k_x = \frac{4k_f\,(1-\sigma)^2\,\Theta_{pm}^2\,x_0}{k_{mf}^2} \quad \text{and} \quad k_i = \frac{\left[4k_f\,(1-\sigma)^2\,\Theta_{pm}\,x_0^2 + \dfrac{8\,l_{pm}\,\Theta_{pm}\,x_0\,(1-\sigma)}{\mu_0\mu_{pm}A_{pm}}\right]}{k_{mf}^2}w \quad .$$

The design of the pre-magnetisation is critical for the maximum attainable control force; e.g. the maximum attainable control force of the presented actuator is about 5 times as high as that of an actuator of the same size but with a pre-magnetisation generated by coils.

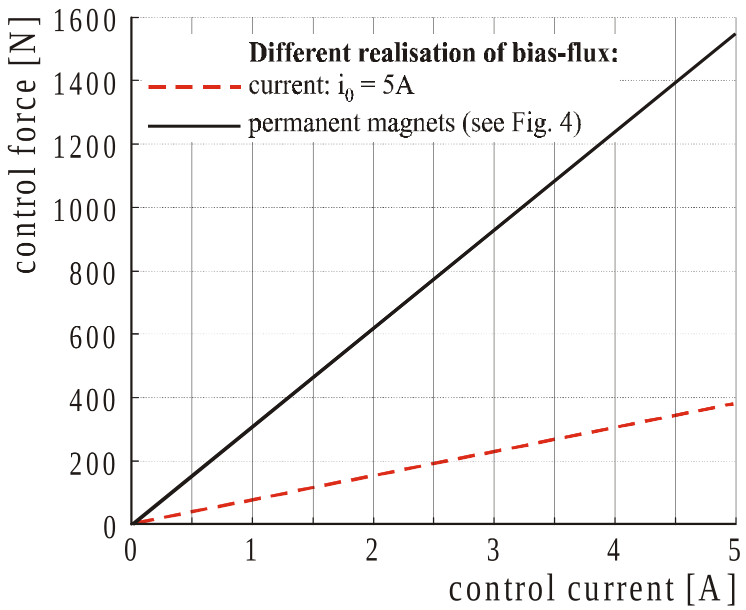

Figure 5- Measured force-current diagram for various magnetic actuators in the reference position x = 0.

The design of the premagnetization is critical for the maximum attainable control forces. In Figure 5 the control force F_m of the actuator shown in Figure 4 is plotted as a function of the control current for the reference position x = 0. As a reference, the maximum attainable control force of an actuator of the same size but with a premagnetization generated by current-carrying coils is given.

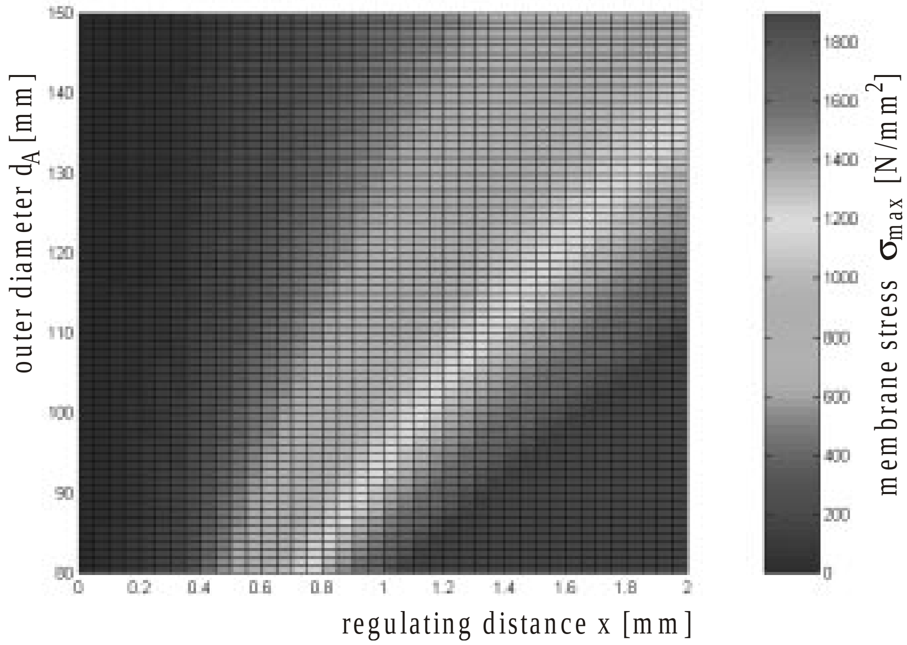

Figure 6- Maximum membrane stress as a function of the outer diameter d_A and the control distance x.

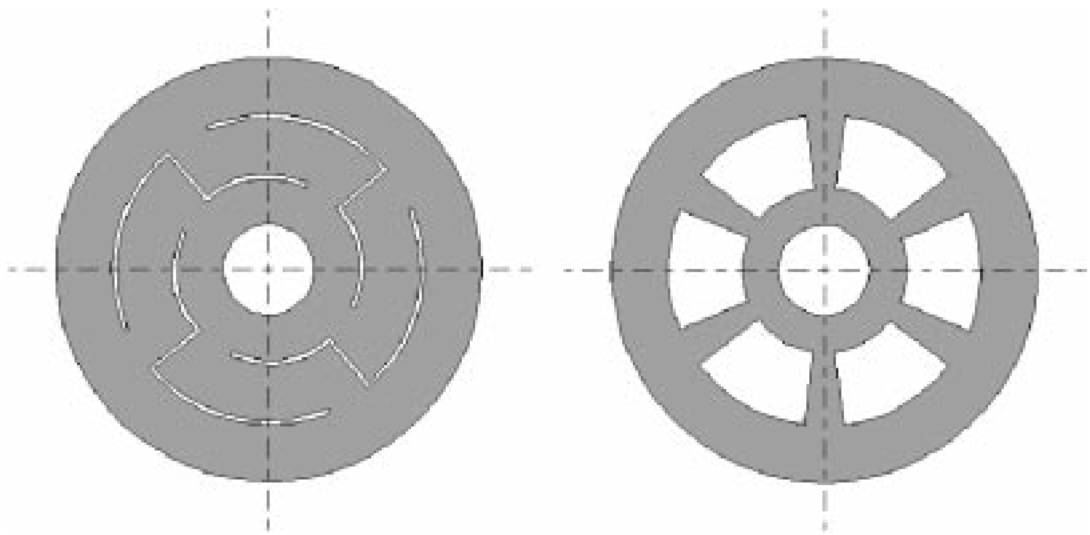

Figure 7- Shapes of membranes with reduced stiffness for higher control distances.

Considering the restoring force due to the stiffness of the membranes k_M yields the force equation:

$$F = (k_x - k_M)x + k_i i. \qquad (6)$$

Very important for the design of the magnetic actuator (as for the hydraulic actuator) are the membranes, that not only determine the air gap but also the maximum attainable control distance. Hence, we briefly explain their design: The feasible control distance depends on the thickness t, the inner diameter d_I and the outer diameter d_A of the membrane. For an inner diameter of $d_I = 25$ mm and a constant membrane thickness, the maximum membrane stress is plotted as a function of the outer diameter of the membrane and the control distance in Figure 6. The maximum stress always occurs at the boundaries of the membrane (here the inner boundary). Given the maximum permissible stress $\sigma_{max} = 1000 N/mm^2$ for the spring steel Ck 85 ($\sigma_{zul} = 1800 N/mm^2$) and a desired control distance of 4 mm ($x = \pm 2$ mm) the outer diameter has to be 140 mm. But the design is not limited to this variation of the membrane thickness and the outer diameter; there also is a great variety of other possible membrane shapes. Two examples are given in Figure 7.

An important parameter in the membrane design is the membrane stiffness k_M. It was found that this stiffness usually is not constant but increases with the displacement. By an adequate design, this can be exploited for a partial compensation of the also nonlinear negative stiffness of the magnetic forces. To this end $k_M(x) = k(x)$ should hold, if possible, but by means of an internal control circuit (nonlinear feedback of x, $\dot{x}$ carried out on the DSP), the remaining deviations can also be removed if necessary and the system, which is at a point of an unstable equilibrium before, can thus be stabilised.

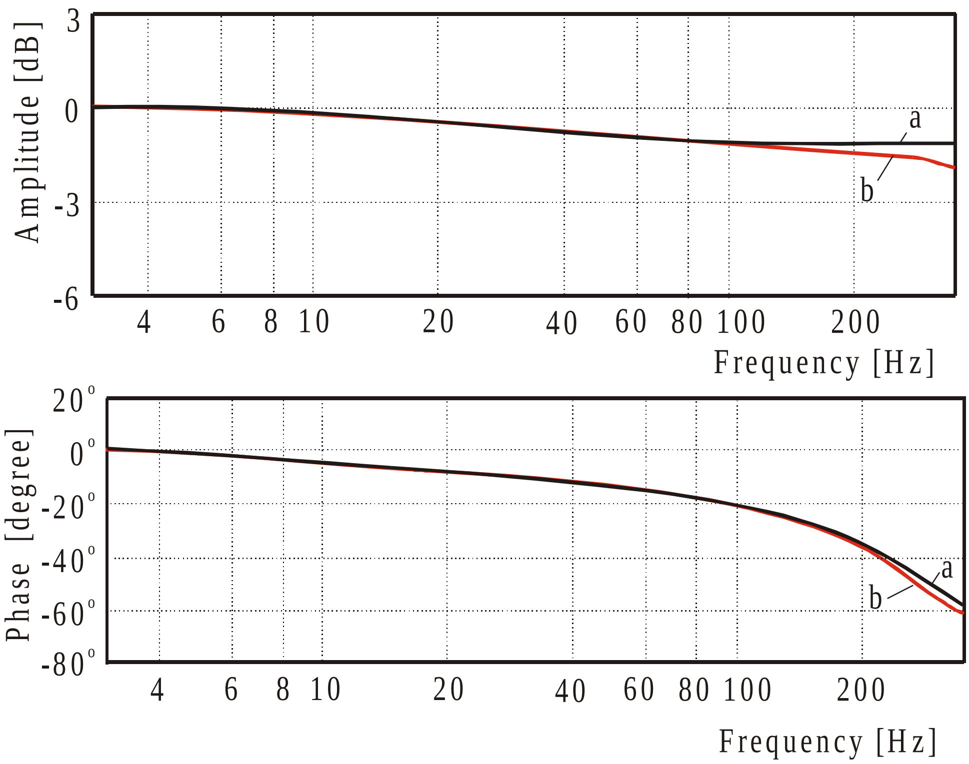

Figure 8- Amplitude and phase response of the magnetic actuators force for two different input currents: $i(t) = i_S \sin(\omega t)$; a) $i_S = 1{,}5$ A, b) $i_S = 3$ A.

The successful integration of an actuator into a closed control loop greatly depends on the dynamic behaviour of the actuator. Hence, the transfer characteristic is most important. Figure 8 shows for the prototype actuator the frequency response Bode-plots of the actuator's control force (system output) for two different control currents $i(t) = i_S \sin(\omega t)$. This input for the actuators was generated by a power amplifier serving as a current source.

As can be seen in Figure 8, the influence of the control current becomes evident only for frequencies beyond 100 Hz. Losses due to hysteresis can be further reduced by using the soft magnetic material Permenorm 5000 (solid). Due to the solid design of the magnetic cores, however, the generation of eddy currents cannot be avoided (in spite of the resistance being three times higher in Permenorm 5000 than in St 37). This leads to a phase lag of already 40° at a frequency of 200 Hz. Improvements can be expected both from new soft magnetic materials and the use of laminated materials instead of a solid design.

4. SUMMARY

The advance of electronics in combination with automatic control technology will further continue. To account for these new developments a practically oriented design of problem-specific actuators is of high importance. In this paper two actuators were presented, one being based upon a hydraulic, the other one upon a magnetic principal. The main objectives of the development process were: Regulating distances in the mm-range, high control forces, good transfer characteristics and small sizes. Whereas the magnetic actuators have a better dynamic behaviour, hydraulic actuators of approximately the same size excel by control forces that are about 10 times higher. The development procedures up to the experimental verifications of the prototypes have been presented. The iterative design work revealed that by a careful design and suitable parameter combinations a great variety of different actuator properties can be achieved providing a great flexibility for widely differing future applications. Considering the rapidly increasing number of applications, a worthwhile objective of future research activities is the provision of systematic development tools for a tailored actuator design.

REFERENCES

[1] Ulbrich, H.; Bormann, J.: Innovative Hydraulic and Magnetic Actuators for Mechanical Engineering Applications. Proceedings of the Int. Symposium on Dynamic Problems of Mechanics and Mechatronics, Ulm, Germany, July 11-16, 1999, pp. 127-134.

[2] Ulbrich, H.; Althaus, J.: Aktive Schwingungsdämpfer für Rotorsysteme. In VDI Berichte Nr. 695, 1988, pp. 129-144.

[3] Ulbrich, H.; Bormann, J.: Hochdynamische hydraulische und magnetische Aktoren für den Maschinenbau. In VDI Fortschritt-Berichte, Reihe 8, Nr. 743, 1999.

[4] Firma Moog: Servoventile der Baureihe 769. Katalog D 769-09.92, Moog GmbH, Böblingen, Deutschland.

[5] Bormann, J.; Ulbrich, H.: Isolation of Vibrations to Avoid Dynamic Interactions between a Telescope and its Foundation by Active Control. Proceedings of the 3rd International Conference on Motion and Vibration Control, Chiba, Japan, September 1-6, 1996, pp. 88-93.

[6] Wang, Y.X.: Berechnung und Auslegung von Magnetstellgliedern mit Strom-Vormagnetisierung und mit Permanent-Vormagnetisierung. Dissertation, Shaker-Verlag, Berichte aus dem Maschinenbau, Aachen, 1996.